MICROCOPY RESOLUTION TEST CHART

NATIONAL BUREAU OF STANDARDS 1963 A

Mechanics and Materials Center
TEXAS A&M UNIVERSITY
College Station, Texas

THE DYNAMIC ENERGY RELEASE RATE FOR A STEADILY
PROPAGATING ANTI-PLANE SHEAR CRACK IN A
LINEARLY VISCOELASTIC BODY

JAY R. WALTON

MM 4867-86-3   JANUARY 1986

86   3   19   105

ADA 165654

REPORT DOCUMENTATION PAGE

1a. REPORT SECURITY CLASSIFICATION unclassified	1b. RESTRICTIVE MARKINGS
2a. SECURITY CLASSIFICATION AUTHORITY	3. DISTRIBUTION/AVAILABILITY OF REPORT
2b. DECLASSIFICATION/DOWNGRADING SCHEDULE	unlimited

4. PERFORMING ORGANIZATION REPORT NUMBER(S) MM-4867-86-3	5. MONITORING ORGANIZATION REPORT NUMBER(S)

6a. NAME OF PERFORMING ORGANIZATION Mechanics & Materials Ctr. Texas A&M University	6b. OFFICE SYMBOL (If applicable)	7a. NAME OF MONITORING ORGANIZATION ONR

6c. ADDRESS (City, State and ZIP Code) College Station, Texas 77843	7b. ADDRESS (City, State and ZIP Code)

8a. NAME OF FUNDING/SPONSORING ORGANIZATION ONR	8b. OFFICE SYMBOL (If applicable)	9. PROCUREMENT INSTRUMENT IDENTIFICATION NUMBER Contract N00014-83-K-0211

8c. ADDRESS (City, State and ZIP Code) Mechanics Division
Office of Naval Research/Code 432
800 N. Quincy Street
Arlington, VA 22217

10. SOURCE OF FUNDING NOS.			
PROGRAM ELEMENT NO	PROJECT NO.	TASK NO	WORK UNIT NO.
			064-520

11. TITLE (Include Security Classification) The Dynamic Energy Release Rate for a Steadily Propagating Anti-Plane Shear Crack in a Linearly Viscoelastic Body

12. PERSONAL AUTHOR(S)
Jay R. Walton

13a. TYPE OF REPORT Technical	13b. TIME COVERED FROM _____ TO _____	14. DATE OF REPORT (Yr., Mo., Day) January 1986	15. PAGE COUNT 22

16. SUPPLEMENTARY NOTATION

17. COSATI CODES			18. SUBJECT TERMS (Continue on reverse if necessary and identify by block number)
FIELD	GROUP	SUB. GR.	Viscoelasticity Dynamic Fracture
			Crack Growth,
			Fracture Mechanics,

19. ABSTRACT (Continue on reverse if necessary and identify by block number)

The steady-state propagation of a semi-infinite, anti-plane shear crack is reconsidered for a general, infinite, homogeneous and isotropic linearly viscoelastic body. As with an earlier study, the inertial term in the equation of motion is retained and the shear modulus is only assumed to be positive, continuous, decreasing and convex. A Barenblatt type failure zone is introduced in order to cancel the singular stress, and a numerically convenient expansion for the dynamic Energy Release Rate (ERR) is derived for a rather general class of crack face loadings. The ERR is shown to have a complicated dependence on crack speed material properties with significant qualitative differences between viscoelastic and elastic material. The results are illustrated with numerical calculations for both power-law material and a standard linear solid.

20. DISTRIBUTION/AVAILABILITY OF ABSTRACT UNCLASSIFIED/UNLIMITED ☒ SAME AS RPT. ☐ DTIC USERS ☐	21. ABSTRACT SECURITY CLASSIFICATION unclassified

22a. NAME OF RESPONSIBLE INDIVIDUAL Dr Alan Kushner	22b. TELEPHONE NUMBER (Include Area Code) (202) 696-4305	22c. OFFICE SYMBOL

DD FORM 1473, 83 APR   EDITION OF 1 JAN 73 IS OBSOLETE.   unclassified

The Dynamic Energy Release Rate for a Steadily Propagating Anti-plane
Shear Crack in a Linearly Viscoelastic Body

by
Jay R. Walton
Department of Mathematics
Texas A&M University
College Station, Texas 77840

DTIC
S ELECTE D
MAR 2 0 1986

B

QUALITY
INSPECTED
3

Accession For

DTIS

By
Distribution/

Availability Codes

Avail and/or
Dist   Special

A-1

Abstract. The steady-state propagation of a semi-infinite, anti-plane shear crack is reconsidered for a general, infinite, homogeneous and isotropic linearly viscoelastic body. As with an earlier study, the inertial term in the equation of motion is retained and the shear modulus is only assumed to be positive, continuous, decreasing and convex. A Barenblatt type failure zone is introduced in order to cancel the singular stress, and a numerically convenient expansion for the dynamic Energy Release Rate (ERR) is derived for a rather general class of crack face loadings. The ERR is shown to have a complicated dependence on crack speed and material properties with significant qualitative differences between viscoelastic and elastic material. The results are illustrated with numerical calculations for both power-law material and a standard linear solid.

§1   Introduction

A central issue in fracture mechanics is the development of fracture criteria. A great many experimental and analytical studies have addressed this topic in the nearly sixty years since Griffith's pioneering work. One fact that has emerged from this effort is that the choice of a fracture criterion is very much dependent upon the particular scenario considered. For example, the notion of a critical Stress Intensity Factor (SIF) has provided a highly successful criterion for quasi-static crack propagation in linearly elastic material. Important factors for the success of the SIF in this setting are that it is often easily computed and that the Energy Release Rate (ERR) can be determined in a simple manner from it. However, such is not the case for dynamically propagating cracks in viscoelastic material for which the entire deformation history during crack advance, not just the SIF, is required in order to calculate the ERR.

The notion of ERR employed here provides a phenomenologically meaningful and mathematicaly convenient fracture criterion for dynamic viscoelastic crack propagation. For dynamic fracture in linearly elastic material, the ERR, G, is usually defined as the difference between the total power input to the body by external forces, P, and the rate of change of the total internal strain energy, $\dot{E}$, and kinetic energy, $\dot{K}$. It is then easily shown (see [1] for example) that G can be calculated from a knowledge of the instantaneous, singular asymptotic stress field at each crack tip.

For viscoelastic material the situation is more complicated. In this case the difference $P-\dot{E}-\dot{K}$ contains two terms: a history dependent body

term, W, representing the energy dissipated through viscous effects and the quantity G which now depends upon the entire history of the singular asymptotic stress and strain fields at each crack tip during the time the tip is advancing. Physically it is reasonable to assume that a fracture criterion should depend only upon these near tip fields. However, the quantity G, which can be interpreted as the power input to the crack tip, is extremely cumberson to calculate from the singular fields. Instead, in this paper a Barenblatt type failure or process zone is introduced behind the crack tip in order to cancel the singular asymptotic fields in front of the crack. What results is that G is given by the formula (3) below and hence that the power input to the crack tip is given by the rate of work done by the tractions in the failure zone.

The purpose of this paper is to demonstrate that for dynamic crack propagation in linear viscoelastic material, the ERR can be conveniently calculated even though it is not just a simple function of the SIF. Moreover, while the SIF is a monotomically decreasing function of crack speed, the ERR can exhibit much more complicated behavior depending upon combined viscoelastic and dynamic effects. In particular, the numerical calculations presented here suggest that for some ranges of crack speed, stable crack growth occurs while for other values, unstable propagation can be expected. This point is considered further when the numerical examples are discussed.

The specific boundary value problem considered here is that corresponding to the steady propagation (to the right) with speed V of a semi-infinite, anti-plane shear crack in a general, homogeneous and isotropic, linearly viscoelatic body. The shear modulus, $\mu(t)$, is assumed only to be a positive, non-increasing and convex function of time, t. The governing equation of motion for the out of plane displacement, u_3, is

$$\mu^* d\Delta u_3 = \rho\, u_{3,tt}$$

where Δ is the two-dimensional Laplacian, $\Delta = (\partial^2/\partial x_1^2) + (\partial^2/\partial x_2^2)$, and μ^* dϵ denotes the Riemann-Stieltjes convolution

$$\mu^* \, d\epsilon = \int_{-\infty}^{t} \mu(t-\tau)\, d\epsilon(\tau) \ .$$

Upon adoption of the Galilean variables $x = x_1 - Vt$, $y = x_2$, the boundary conditions may be written

$$\sigma_{23}(x,0) = \frac{\partial}{\partial y} (\mu^* \, du_3) = f(x), \quad x < 0$$

$$u_3(x,0) = 0 , \qquad\qquad\qquad x > 0$$

$$\sigma_{ij}(x,y) \to 0, \qquad\qquad x^2 + y^2 \to \infty$$

where σ_{ij} are the stress components and $f(x)$ is a system of tractions moving with the crack.

The starting point of the present investigation is the solution derived in [3] for the above boundary value problem. It was shown in [3] that two cases arise naturally in constructing the solution: $0 \leq V < C^*$ and $C^* < V < C$ where $C^* = (\mu(\infty)/\rho)^{1/2}$ and $C = (\mu(0)/\rho)^{1/2}$ are the elastic shear wave speeds corresponding to the equilibrium and glassy values of

the shear modules $\mu(t)$. For $0 \leq V < C^*$, the stress field is that for static elastic fracture and is therefore independent of crack speed and material properties. Whereas, for $C^* < V < C$, the stress field is both speed and material dependent. Specifically, the SIF, K, is given by

$$K = \begin{cases} \frac{-1}{\pi} \int_{-\infty}^{0} \sigma_{23}^{-}(x,0) \, |x|^{\frac{-1}{2}} \, dx \quad , \quad 0 \leq V < C^* & (1) \\ \\ -\frac{1}{\pi} \int_{-\infty}^{0} \sigma_{23}^{-}(x,0) \, |x|^{\frac{-1}{2}} \, e^{q_0 x} \, dx \quad C^* < V < C \end{cases}$$

where $g^{-}(x)$ ($g^{+}(x)$) denotes the restriction of $g(x)$ to $x < 0$ ($x < 0$) and q_0 is the unique positive constant such that

$$V q_0 \int_{0}^{\infty} \mu^*(t) e^{-q_0 V t} \, dt = (V/C)^2 \quad . \tag{2}$$

In (2), $\mu^*(t)$ denotes the nondimensional modulus given by

$$\mu^*(t) = \mu(t)/\mu(0).$$

In order to calculate the ERR, the object of principal interest in the present study, it is necessary, as discussed earlier, to modify the above boundary value problem by the introduction of a Barenblatt type failure zone. Specifically, it is now assumed that two loads are acting on the crack faces: the applied (external) tractions $\sigma_{23}^{-}(x,0)$ discussed above, but now denoted $\sigma_{e}^{-}(x)$, and cohesive (failure) stresses $\sigma_{f}^{-}(x)$ acting in a failure zone of length a_f immediately behind the crack tip. The only assumptions about $\sigma_{f}^{-}(x)$ are that a_f is small relative relative to some length scale a_e associated with $\sigma_{e}^{-}(x)$ and that

$K_e + K_f = 0$ where K_e and K_f are the SIF's corresponding to

σ_e^- and σ_f^-, respectively. Hence the effect of the failure zone is to

cancel the singular stresses ahead of the crack tip and thereby produce

a cusp shaped crack profile behind the tip.

The ERR, G, for steady-state crack propagation is now defined by

$$G = \int_{-a_f}^{0} \sigma_f^-(x)\, u_{3,1}^-(x,0)dx \tag{3}$$

where $u_3(x,0)$ is the crack face displacement corresponding to the combined

loading $\sigma_e^- + \sigma_f^-$. Thus G has the interpretation of power input to the

crack tip from the total load, i.e. the power available to the crack

tip for propagating the crack. Unlike for elastic material, G for

viscoelastic material is not merely a simple function of K. Rather, as is

evident from [3], $u_{3,1}^-(x,0)$ has a complicated dependence upon the loading

$\sigma_e^-(x,0)$, making impracticable the direct numerical evaluation of (3). In

the next section, a computationally convenient expression for (3) is

derived for a special, but still fairly general, class of loadings

σ_e^- and σ_f^-.

§2. The Calculation of G

For simplicity of argument and clarity of result, the ERR, G, given

in (3) will be calculated first for a simple special case. Specifically,

the external load, $\sigma_e^-(x)$ and failure zone stresses, $\sigma_f^-(x)$ will be assumed

to have the forms

$$\sigma_e^-(x) = L_e \; e^{x/a_e}$$

$$-\infty < x < 0 \qquad\qquad (4)$$

$$\sigma_f^-(x) = - L_f \; e^{x/a_f}$$

where $a_f/a_e \ll 1$. (c.f. [2]) For a_f/a_e small enough, the fact that $\sigma_f^-(x)$ does not have support in some small, compact interval behind the crack tip will have a negligible effect on the results. The assumptions (4) then clearly incorporate the salient features of the Barenblatt model, namely, a set of cohesive stresses and associated length scale a_f and a length scale a_e associated with the applied load α_e^- such that α_f^- cancels the singular stresses produced by σ_e^- and $a_f/a_e \ll 1$. If should be noted that in this case, (3) is replaced by

$$G = \int_{-\infty}^{0} \sigma_f^-(x) \; u_{3,1}^-(x,0)dx. \qquad\qquad (5)$$

In order to present the results in a suitable nondimensional form, it is useful to introduce certain parameters. First a characteristic time scale, τ, is defined and the shear modulus given the form

$$\mu(t) = \mu_\infty \; m(t/\tau)$$

where $m(s)$ is a nondimensional function of s with $\lim_{s \to \infty} m(s) = 1$ and $\mu_\infty = \lim_{t \to \infty} \mu(t)$. Also useful are the nondimensional parameters α, β, γ, ϵ and λ defined by

$$\alpha \equiv C^*\tau/a_e \quad \beta \equiv q_0 a_e \quad \gamma \equiv V/C^* \quad \epsilon \equiv a_f/a_e \quad \lambda \equiv L_f/L_e. \qquad (6)$$

It should be noted that α and β assume any positive value while γ must be such that $0 < \gamma < C/C^*$. Also, $\beta = 0$ whenever $0 < V \leq C^*$.

The desired expression for G is most easily expressed in terms of the Carson transform, $\overline{m}(s)$, of $m(t)$ defined by

$$\overline{m}(s) = m(0) + \int_0^\infty e^{-ts} \, dm(t).$$

It is useful to record for future reference the easily derived formula

$$\overline{\mu}(r) = \mu_\infty \overline{m}(r\tau).$$

It will now be shown that for loads of the form (4), G is given by

$$G = \frac{K^2}{2\mu_\infty} \left(\frac{1-\epsilon}{1+\epsilon}\right) \frac{1}{\overline{m}(\alpha\gamma/\epsilon)} \left[\frac{1-(\beta\epsilon)^2}{1-\gamma^2/\overline{m}(\alpha\gamma/\epsilon)}\right]^{\frac{1}{2}} \tag{7}$$

where $K = K_e = -K_f$ is the dynamic SIF. From (1) and (4) it follows easily that

$$K = \frac{L_f \sqrt{a_f}}{\sqrt{1+\beta\epsilon}} = \frac{L_e \sqrt{a_e}}{\sqrt{1+\beta}} . \tag{8}$$

The derivation of (7) from (5) utilizes the Fourier transform $\hat{f}$ of a function f. Specifically,

$$\hat{f}(p) = \int_{-\infty}^\infty f(x) \, e^{ixp} dx$$

with inverse, $f(x)$, given by

$$f(x) = \frac{1}{2\pi} \int_{-\infty}^\infty f(p) \, e^{-ixp} dp.$$

Applying the Parseval formula for the Fourier transform, it follows from (5) that

$$G = \int_{-\infty}^\infty \sigma_{\overline{f}}(p)\hat{u}_{3,1}(p) dp. \tag{9}$$

In consideration of (4), a straight forward calculation shows that

$$\hat{\sigma}_f^-(p) = \frac{-a_f L_f}{(1+ia_f p)}$$

(10)

$$\sigma_f^-(p) = \frac{-a_f L_f}{2\pi(1-ia_f p)} \; .$$

The integral in (9) may be readily evaluated using residues since, from (10), it is clear that $\sigma_f^-(p)$ has a meromorphic extension to the lower complex half-plane with a simple pole at $-i/a_f$. Moreover, $u_{3,1}(x,0)$ vanishes for $x > 0$ from which it follows that $\hat{u}_{3,1}(p) = u_{3,1}^-(p)$ has an analytic extension, $F^-(z)$, to the lower half-plane with

$$\lim_{q\to\infty} F^-(p-iq) = 0.$$

Consequently, for G one has

$$G = L_f F^-(-i/a_f).$$

(11)

It remains to evaluate $F^-(-i/a_f)$. To this end use will be made of the following formulas derived in [3]:

$$\hat{u}_{3,1}(p) = \hat{\sigma}(p)/G(p),$$

(12)

$$G(p) = - i \; \text{sgn}(p) \; \overline{\mu}(iVp)\gamma_1(iVp),$$

(13)

and

$$\gamma_1(ipV) = (1-\gamma^2/\overline{\mu}(iVp))^{1/2} \; .$$

(14)

Here one has

$$\hat{\sigma}(p) = \hat{\sigma}^-(p) + \hat{\sigma}^+(p)$$

$$\sigma^-(x) = \sigma_e^-(x) + \sigma_f^-(x)$$

where $\sigma^+(x)$ $(\sigma^-(x))$ denotes the restriction of $\sigma(x)$ to the half-line $x > 0$ $(x < 0)$. It should be noted that $\sigma^+(x)$ is the nonsingular stress field ahead of the crack that results from superposing σ_e^- and σ_f^-. Moreover, it is shown in [3] that

$$\hat{\sigma}^+(p) = \lim_{I_m(z) \to 0+} F^+(z)$$

where

$$F^+(z) = (q_0 - iz)^{1/2} \frac{1}{2\pi i} \int_{-\infty}^{\infty} \hat{\sigma}^-(\tau)(q_0 - i\tau)^{-1/2} \frac{d\tau}{(\tau - z)} , \qquad (15)$$

with q_0 given in (2). To evaluate (15), consider first

$$\hat{\sigma}_e^+(p) = \lim_{I_m(z) \to 0+} F_e^+(z) ,$$

in which

$$F_e^+(z) = -(q_0 - iz)^{1/2} \frac{1}{2\pi i} \int_{-\infty}^{\infty} \hat{\sigma}_e^-(\tau)(q_0 - i\tau)^{-1/2} \frac{d\tau}{(\tau - z)} . \qquad (16)$$

From the analog of (10) for $\hat{\sigma}_e^-(p)$, one sees that $\hat{\sigma}_e^-(p)$ has a simple pole at i/a_e. Since the branch of $(q_0 - i\tau)^{-1/2}$ must be chosen to be analytic in the upper half-plane (see [3]), the integral in (16) can be calculated using residues. Thus for $I_m(z) > 0$,

$$F_e^+(z) = -(q_0 - iz)^{1/2}[-iL_e(q_0 + 1/a_e)^{-1/2}/(i/a_e - z) + \hat{\sigma}_e^-(z)(q_0 - iz)^{-1/2}].$$

Now letting $I_m(z) \to 0$ and adding $\hat{\sigma}^-(p)$ to $\hat{\sigma}^+(p)$ there results

$$\hat{\sigma}_e(p) = F^+(p) + \hat{\sigma}^-(p)$$

$$= i L_e(q_0 - ip)^{1/2}(q_0 + 1/a_e)^{-1/2}/(i/a_e - p)$$

$$= a_e L_e(\beta/(1 + \beta))^{1/2}(1 - ip/q_0)^{1/2}/(1 + ipa_e). \qquad (17)$$

Similarly, for $\hat{\sigma}_f(p)$ one can show that

$$\hat{\sigma}_f(p) = -a_f L_f (\beta\epsilon/(1+\beta\epsilon))^{1/2}(1-i\,p/q_0)^{1/2}/(1+ipa_f). \qquad (18)$$

Combining (4), (8), (17) and (18) one concludes that

$$\hat{\sigma}(p) = -a_e L_e (\beta/(1+\beta))^{1/2}\frac{(1-\epsilon)(1-ip/q_0)^{1/2}}{(1+ia_e p)(1+ia_f p)}\quad. \qquad (19)$$

Substitution of (19) into (12) gives

$$F^-(p) = \hat{u}_{3,1}(p) = a_e L_e (\beta/(1+\beta))^{1/2}\,(1-\epsilon)\Phi_1(p)\Phi_2(p)$$

with

$$\Phi_1(p) = (1+ia_e p)^{-1}(1+ia_f p)^{-1}$$

and

$$\Phi_2(p) = (1-ip/q_0)^{1/2}/G(p).$$

$\Phi_1(p)$ is obviously an analytic function in the lower half-plane and in [3]

it was shown that the branches of $(1-ip/q_0)^{1/2}$ and $\gamma_1(iVp)$ must be chosen

so that $\Phi_2(p)$ is also analytic there. Thus one may substitute (20) into

(11) making use of (13) and (14) to conclude that

$$G = a_e L_e L_f \frac{(\beta/(1+\beta))^{1/2}(1-\epsilon)}{2(1+a_e/a_f)\bar{\mu}(V/a_f)}\left[\frac{1-1/(q_0 a_f)}{1-\gamma^2/\bar{m}(V/a_f)}\right]^{1/2}\quad.$$

Combining (6), (8), and (21), there finally results the desired formula
(7).

The derivation given above is easily modified to produce an analog to

formula (7) for more general loads of the form

$$\sigma_e^-(x) = L_e \int_0^\infty e^{tx/a_e} \, d \, h_e(t)$$

$$\sigma_f^-(x) = -L_f \int_0^\infty e^{tx/a_f} \, d \, h_f(t)$$

(22)

where $h_e(t)$ and $h_f(t)$ are arbitrary signed (not necessarily positive) measures restricted only to the extent that the required integrals converge. For example, the special cases (4) correspond to $d \, h_e(t) = d \, h_f(t) = \delta(t-1)$, the Dirac measure concentrated at $t = 1$. As further examples, $d \, h_e(t) = \sin(t)dt$ and $d \, h_e(t) = \cos(t)dt$ produce

$$\sigma_e^-(x) = \frac{1}{1+(x/a_e)^2} \quad \text{and} \quad \sigma_e^-(x) = \frac{(x/a_e)}{1+(x/a_e)^2} \quad ,$$

respectively.

Substitution of (22) into (1) followed by an interchange of order of integration results in

$$K_e = L_e \sqrt{a_e} \int_0^\infty (t+\beta)^{-1/2} \, d \, h_e(t)$$

$$= L_f \sqrt{a_f} \int_0^\infty (t+\epsilon\beta)^{-1/2} \, d \, h_f(t)$$

$$= - K_f$$

where, as before, $\beta \equiv a_e q_0$. Corresponding to (10) there is

$$\hat{\sigma}_e^-(p) = a_e L_e \int_0^\infty (t+ipa_e)^{-1} d \, h_e(t)$$

(23)

$$\sigma_e^-(p) = \frac{a_e L_e}{2\pi} \int_0^\infty (t-ia_e p)^{-1} d \, h_e(t) \ .$$

Lines (15) and (16) are still valid but with $\hat{\sigma}_e^-$ given now by (23). In

particular, one has for $I_m(z) > 0$ and after an interchange of integration

that

$$F_e^+(z) = -(q_0-iz)^{1/2} \frac{1}{2\pi i} a_e L_e \int_0^\infty dh_e(\tau) \int_{-\infty}^\infty (q_0-it)^{-1/2}(\tau+ita_e)^{-1} \frac{dt}{(t-z)} \quad . \quad (24)$$

The integrand in the inner integral in (24) is analytic for $I_m(t) > 0$

except for simple poles at $t = i\tau/a_e$ and $t = z$. Calculating the inner

integral by residues, there then results

$$\frac{1}{2\pi i} \int_{-\infty}^\infty (q_0-it)^{-1/2}(\tau+i\,ta_e)^{-1} \frac{dt}{(t-z)} = [(q_0-iz)^{-1/2}-(q_0+\tau/a_e)^{-1/2}]/(\tau+iza_e) .$$

If one now lets $I_m(z) \to 0$ in this last result and makes use of (23a) and

(24) it follows that

$$\hat{\sigma}_e(p) = \hat{\sigma}_e^+ + \hat{\sigma}_e^- = a_e L_e(1-ip/q_0)^{1/2} \int_0^\infty (\beta/(\tau+\beta))^{1/2} \frac{dh_e(\tau)}{(\tau+ipa_e)} \quad . \quad (25)$$

For $\hat{\sigma}_f(p)$ one has

$$\hat{\sigma}_f(p) = -a_f L_f(1-ip/q_0)^{1/2} \int_0^\infty (\beta\epsilon/(\tau+\beta\epsilon))^{1/2} \frac{dh_f(\tau)}{(\tau+ipa_f)} \quad ,$$

the analog of (18), which when combined with (25), gives

$$\hat{\sigma}(p) = \hat{\sigma}_e(p) + \hat{\sigma}_f(p)$$

$$= (1-i\,p/q_0)^{1/2}H(p) \qquad (26)$$

with $H(p) \equiv \int_0^\infty \frac{a_e L_e(\beta/(\tau+\beta))^{1/2}}{(\tau+ia_e p)} dh_e(\tau) - \int_0^\infty \frac{a_f L_f(\epsilon\beta/(\tau+\epsilon\beta))^{1/2}}{(\tau+ia_f p)} dh_f(\tau).(27)$

It is easily seen that $H(p)$ is analytic for $I_m(p) < 0$ and $H(p) \to 0$ as

$I_m(p) \to -\infty$. After substitution of (11), (12), (23b), (26), and (27) into

(9) and an interchange of integration one obtains

$$G = a_f \, L_f \int_0^\infty dh_f(t) \, \frac{1}{2\pi} \int_{-\infty}^\infty \Psi(t,p) dp \tag{28}$$

where

$$\Psi(t,p) = \frac{H(p)(1-ip/q_0)^{1/2}}{(t-ipa_f)G(p)} \, .$$

As before, the branches of $\gamma_1(ipV)$ and $\sqrt{1-ip/q_0}$ can be chosen so that

$i \, \mathrm{sgn}(p) \, \sqrt{1-i \, p/q_0}/\gamma_1(ipV)$ is analytic for $I_m(p) < 0$. Thus, $\Psi(t,p)$ is

analytic for $I_m(p) < 0$, except for a simple pole at $p = -it/a_f$.

Evaluting the inner integral in (28) by residues, yields finally

$$G = \frac{L_f}{\mu^\infty} \int_0^\infty dh_f(t) \, \frac{H(-it/a_f)}{\overline{m}(\frac{\alpha\gamma t}{\varepsilon})} \left[\frac{1-t/(\beta\varepsilon)}{1-\gamma^2/\overline{m}(\alpha\gamma t/\varepsilon)} \right]^{1/2} \tag{29}$$

with $H(-it/a_f)$ defined in (27).

The two integrations required to evaluate (29) make it much more

cumbersome to calculate numerically than (7), though still much easier

than calculating G directly from either (3) or (5). However, since

$\varepsilon \ll 1$, it is not unreasonable to take $dh_f(t) = \delta(t-1)$, i.e. to take the

simple form (4b) for $\sigma_f^-(x)$, since the details of the failure zone stress

are not significant. Formula (29) then simplifies greatly to

$$G = \frac{L_f}{\mu^\infty} \frac{H(-i/a_f)}{\overline{m}(\alpha\gamma/\epsilon)} \left[\frac{1-1/(\beta\epsilon)}{1-\gamma^2/\overline{m}(\alpha\gamma/\epsilon)} \right]^{1/2}$$

$$H(-i/a_f) = \frac{-a_f L_f}{2} (\epsilon\beta/(1+\epsilon\beta))^{1/2} + a_e L_e \; \beta^{1/2} \int_0^\infty \frac{dh_e(\tau)}{(\tau+1/\epsilon)(\tau+\beta)^{1/2}}$$

subject to the auxiliary constraint

$$L_f(\frac{a_f}{1+\beta\epsilon})^{1/2} = L_e(a_e)^{1/2} \int_0^\infty \frac{dh_e(t)}{(t+\beta)^{1/2}} \; .$$

In the next section, the qualitative behavior of G is investigated by considering the special cases of a power-law material and a standard linear solid.

§3. Numerical Examples

The formula (7) will now be applied to the special cases of a standard linear solid and power-law material. First considered is the standard linear solid, which is modelled by a constant Poisson's ratio and a shear modulus, $\mu(t)$, of the form

$$\mu(t) = \mu_\infty(1+n\,e^{-t/\tau})$$

$$= \mu_\infty m(t/\tau).$$

It follows that $1 + n = (C/C\star)^2$ and $\overline{m}(s)$ is given by

$$\overline{m}(s) = \frac{1+s(1+n)}{(1+s)} \; . \tag{30}$$

From (2) and (30) one easily shows that

$$q_0 = \frac{(\gamma^2-1)}{\tau V((1+n)-\gamma^2)} \; . \tag{31}$$

It should be noted that the restriction $0 < V < C$ corresponds to $0 \le \gamma^2 < 1 + n$, and moreover, that $q_0 = 0$ for $0 \le \gamma \le 1$. From (7), (8),

(13), (30), and (31), one readily obtains the formula

$$G = \frac{a_e L_e^2}{2\mu_\infty} g(\alpha, \gamma, n, \varepsilon)$$

where

$$g(\alpha, \gamma, n, \varepsilon) = \left(\frac{1-\varepsilon}{1+\varepsilon}\right) \frac{(1+\alpha\gamma)}{(1+\alpha\gamma(1+n))^{1/2}(1-\gamma^2+\alpha\gamma(1+n-\gamma^2))^{1/2}} \quad 0 \le \gamma \le 1$$

and

$$(32)$$

$$g(\alpha, \gamma, n, \varepsilon) = \left(\frac{1-\varepsilon}{1+\varepsilon}\right) \frac{(\varepsilon+\alpha\gamma)(1+\beta\varepsilon)^{1/2}}{(1+\beta)(\alpha\gamma(n+1-\gamma^2))^{1/2}(\varepsilon+\alpha\gamma(1+n))^{1/2}} \quad 1 < \gamma < (1+n)^{1/2}.$$

Figure 1 displays a normalized SIF, $k \equiv K/(L_e\sqrt{a_e})$, which from (8) is

seen to be just $k = (1+\beta)^{-1}$. From (31), β is seen to be given by

$$\beta = \frac{(\gamma^2-1)}{\alpha\gamma((1+n)-\gamma^2)}.$$

In Figure 1, k is plotted atainst $\gamma' \equiv \gamma/\sqrt{1+n}$ for $\alpha = .1$, 1 and 10.

Clearly, k must vanish as γ approaches 1.

In Figure 2, $g(\alpha, \gamma, n, \varepsilon)$ is plotted against $\log(\gamma)$ for $0 < \gamma$ 1 and

against $\log((\sqrt{n+1}-1)/(\sqrt{n+1}-\gamma))$ for $1 < \gamma < \sqrt{n+1}$, for $n = 10$, $\varepsilon = .01$ and

$\alpha = .1$, 1, 10,100. Thus the failure zone length is assumed to be

constant. For many materials (such as rubber) a more realistic

approximation is furnished by assuming a constant failure zone stress

level, L_f. This is tantamount to holding λ constant and allowing ε to

vary. From (8) one easily calculates ε as a function of λ to be

$$\varepsilon = [\lambda^2(\beta+1)-\beta]^{-1}.$$

Consequently, one may regard g as a function of α, γ, n and λ.

Figure 3 is the analog of Figure 2 for $\lambda = 10$, $n = 10$ and $\alpha = .1$, 1, 10.

It should be noted that g vanishes as γ approaches $\sqrt{n+1}$ when λ is held

constant. However, with ε constant, g tends to a non-zero finite limit as

γ tends to $\sqrt{n+1}$, i.e. as V approaches the glassy shear wave speed.

Indeed, from (32b) it is easily seen that

$$\lim_{\gamma \to \sqrt{n+1}} g(\alpha,\gamma,n,\varepsilon) = \left(\frac{1-\varepsilon}{1+\varepsilon}\right) \frac{(\varepsilon + \alpha\sqrt{n+1})(\varepsilon/n)^{1/2}}{(\varepsilon + \alpha(n+1)^{3/2})^{1/2}} .$$

The second example considered is a power-law material for which the

shear modulus is assumed to have the form

$$\mu(t) = \mu_\infty (1+(t/\tau)^{-n}) , \quad 0 < n < 1$$

$$= \mu_\infty \, m(t/\tau).$$

For such material, the glassy wave speed, C, is infinite and $\bar{m}(s)$ is given

by

$$\bar{m}(s) = 1 + \Gamma(1-n)s^n . \tag{33}$$

From (2) and (33) one sees that

$$q_0 = \left(\frac{1}{V\tau}\right) \left[\frac{\gamma^2-1}{\Gamma(1-n)} \right]^{1/n}$$

and hence that $\beta = (\gamma^2-1)^{1/n}/(\alpha\gamma)$ $\tag{34}$

where, for convenience, α has been redefined by

$$\alpha = \Gamma(1-n)^{1/n} \, C^\star\tau / a_e .$$

Combining (7), (8), (13), (33), and (34), it may be shown that

$$G = \frac{a_e L_e^2}{2\mu_\infty} g(\alpha,\gamma,n,\varepsilon)$$

where

$$g(\alpha,\gamma,n,\epsilon) = \begin{cases} (\frac{1-\epsilon}{1+\epsilon})[1-\gamma^2+(\alpha\gamma)^n]^{-1/2}[1+(\alpha\gamma)^n]^{-1/2} & 0 < \gamma < 1 \\ \\ (\frac{1-\epsilon}{1+\epsilon})(\frac{1-(\epsilon\beta)^2}{1-(\epsilon\beta)^n})^{1/2}((\alpha\gamma)^{2n}+(\alpha\gamma)^n)^{-1/2}/(1+\beta) & 1 < \gamma \end{cases} \quad .$$

Figure 4 is a plot of the non-dimensional SIF $k = (1+\beta)^{-1}$ against γ for $\alpha=.1$, 1, 10 and $n=.3$. Figure 5 shows g plotted against $\log(\gamma)$ for $\alpha=.1$, 1, 10, 100, $n=.3$, $\epsilon=.01$. Figure 6 has $\alpha=1$, $\epsilon=.01$, $n=.1$, .3, .5, .7. The case λ constant is not exhibited here since it results in little change from the constant ϵ calculations.

Several comments on the numerical results should be made. It can be observed for a standard linear solid in Figures 2 and 3 and may be shown analytically for general material that the slope of the curve g versus γ is discontinuous for $\gamma = 1$, i.e. as V passes through C*. A more striking observation is the loss of monotonicity of g as a function of γ for certain ranges of the parameters. For example, in Figures 2 and 3, it is seen that for $\alpha = .1$, g is monotone decreasing in γ, whereas for $\alpha = 1$, 10 g has a relative maximum on $1 < \gamma < \sqrt{1+n}$. As seen from Figure 6, for power-law material, varying the exponent n also causes a transition from monotonicity to having a single relative maximum. The lack of monotonicity suggests that certain crack speeds are unstable. In particular, since G has the interpretation of power input to the crack tip, the γ-intervals on which g is increasing are those on which an increase in crack speed produces an increase in the power available to propagate the crack. Evidently this lack of monotonicity is due to the combined inertial and dynamics effects considered here. It is also worth noting that these results illustrate that in contrast to elastic material,

for viscoelastic material, there is no simple relationship between G and K. Indeed, though K is always a monotone decreasing function of V which vanishes at the glassy shear wave speed, G need not be monotone and need not vanish at $V = c$.

ACKNOWLEDGEMENT.

REFERENCES

[1] L. B. Freund, "The analysis of elastodynamic crack tip stress fields," in Mechanics Today, vol. 3, ed. S. Nemat-Nasser, Pregamon, 1976, pp. 55-91.

[2] L. B. Sills and Y. Benveniste, "Steady-state propagation of a mode III interface crack between dissimilar viscoelastic media," Ind. J. Eng. Sci., (19), 1981,pp. 1255-1268.

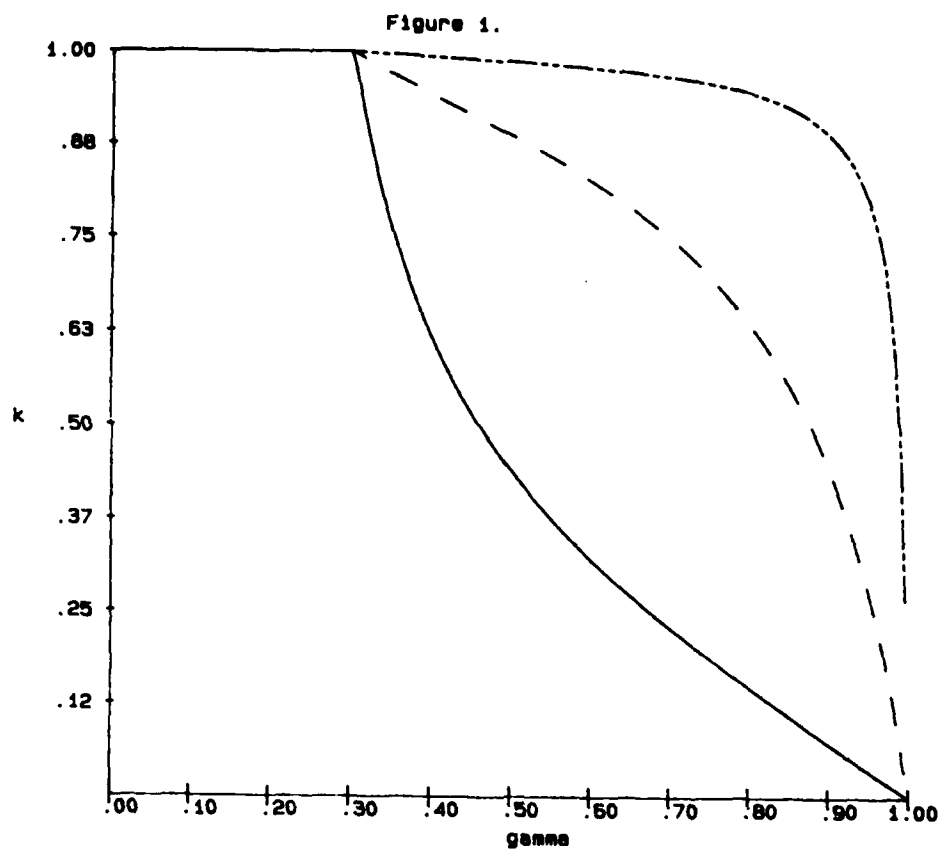[3] J. R. Walton, "On the steady-state propagation of an anti-plane shear crack in an infinite general linearly viscoelastic body," Quart. Appl. Math., April 1982, pp. 37-52.

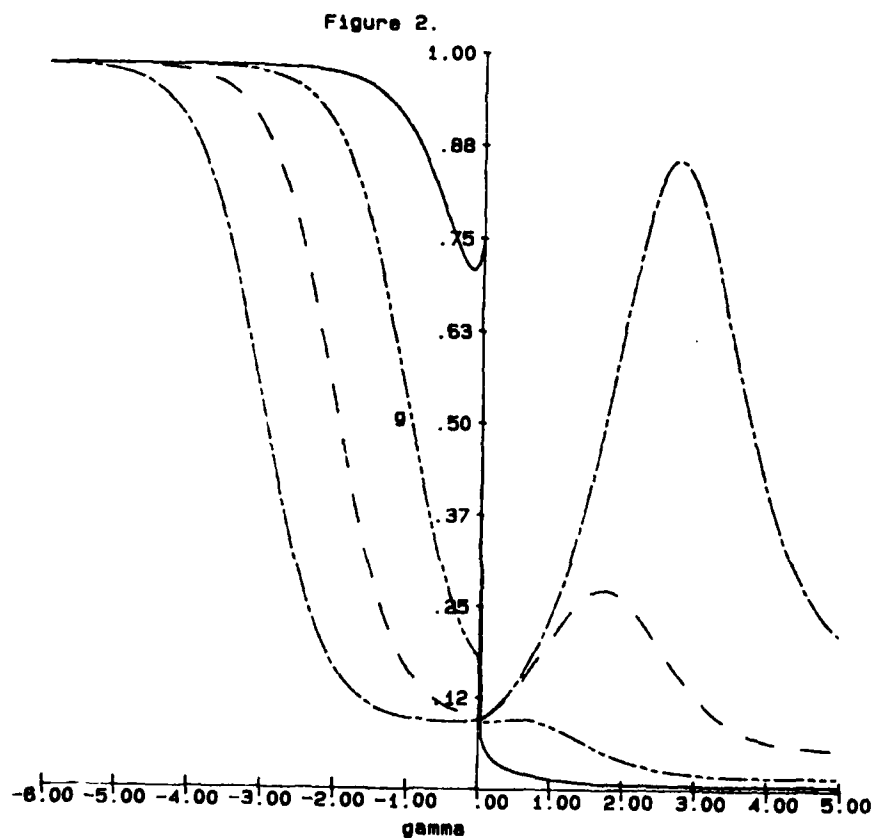Figure 1. k versus $\gamma/(n+1)^{1/2}$ for a standard linear solid with $n=10$ and $\alpha=.1(\text{———})$, $1.0(\text{— — —})$, $10.0(\text{—··—})$.

Figure 2. g versus γ' for a standard linear solid with $n=10$, $\epsilon=.01$, $\alpha=.1(\text{———})$, $1.0(\text{—··—})$, $10.0(\text{— — —})$, $100.0(\text{—— —})$.
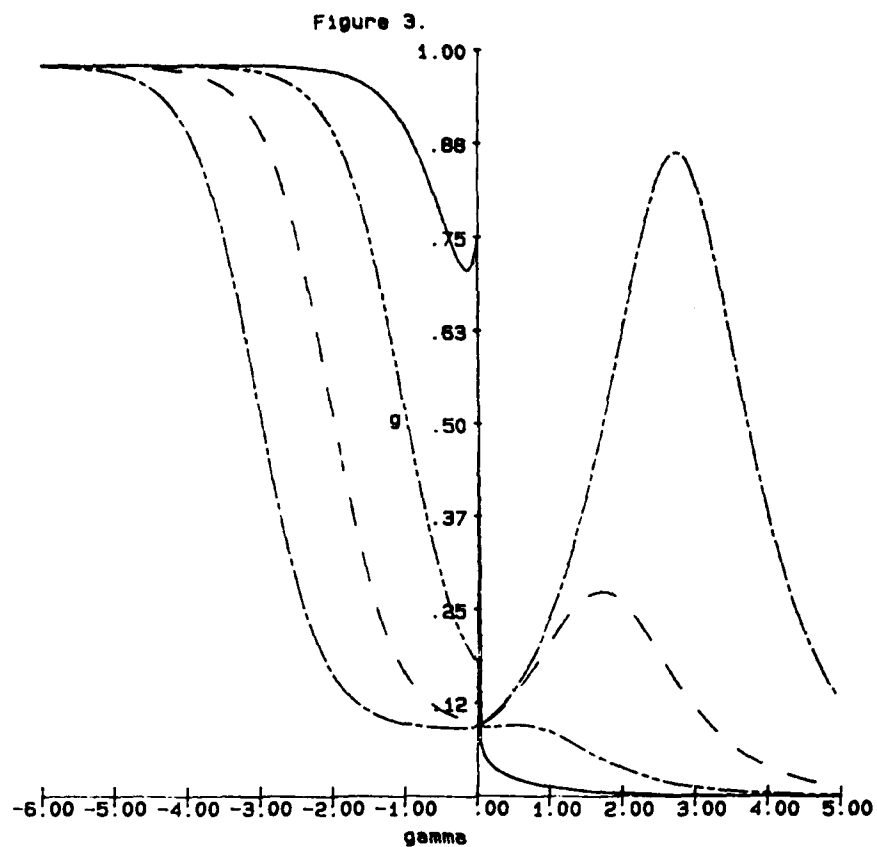
Figure 3.

Figure 3. g versus γ' for a standard linear solid with $\eta = 10$, $\lambda = 10.0$, and $\alpha = .1$(——), 1.0(—··—), 10.0(– – –), 100.0(—·—).
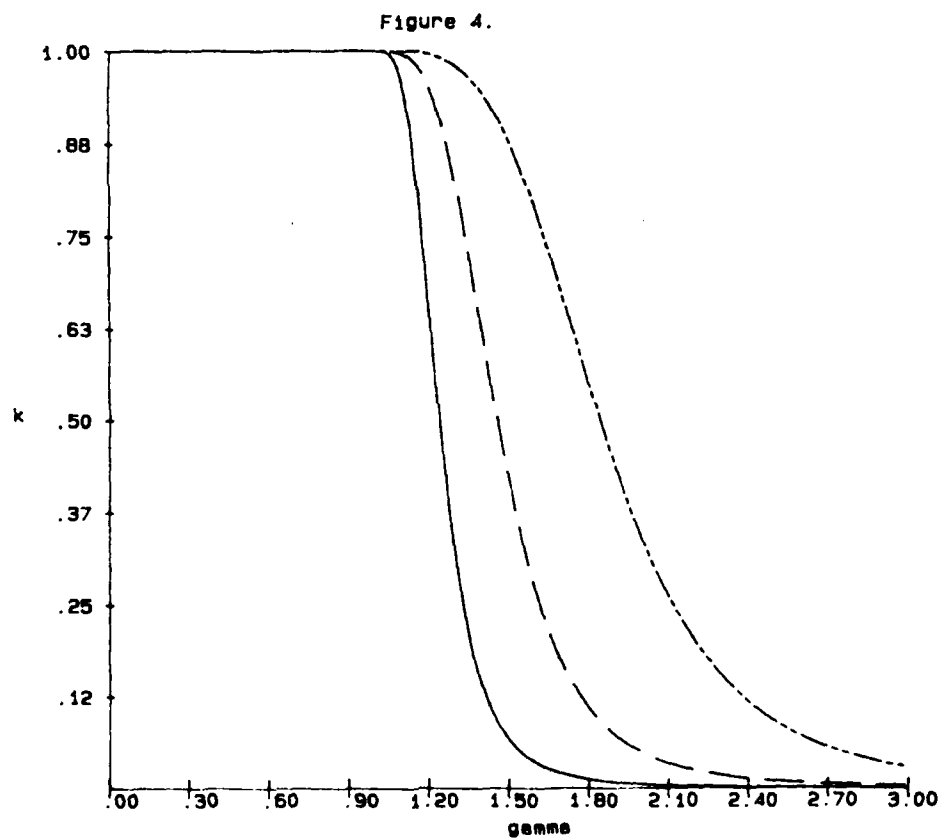
Figure 4.

Figure 4. k versus γ for a power-law material with $n = .3$ and $\alpha = .1$(——), 1.0(– – –), 10.0(—·—).

Figure 5.
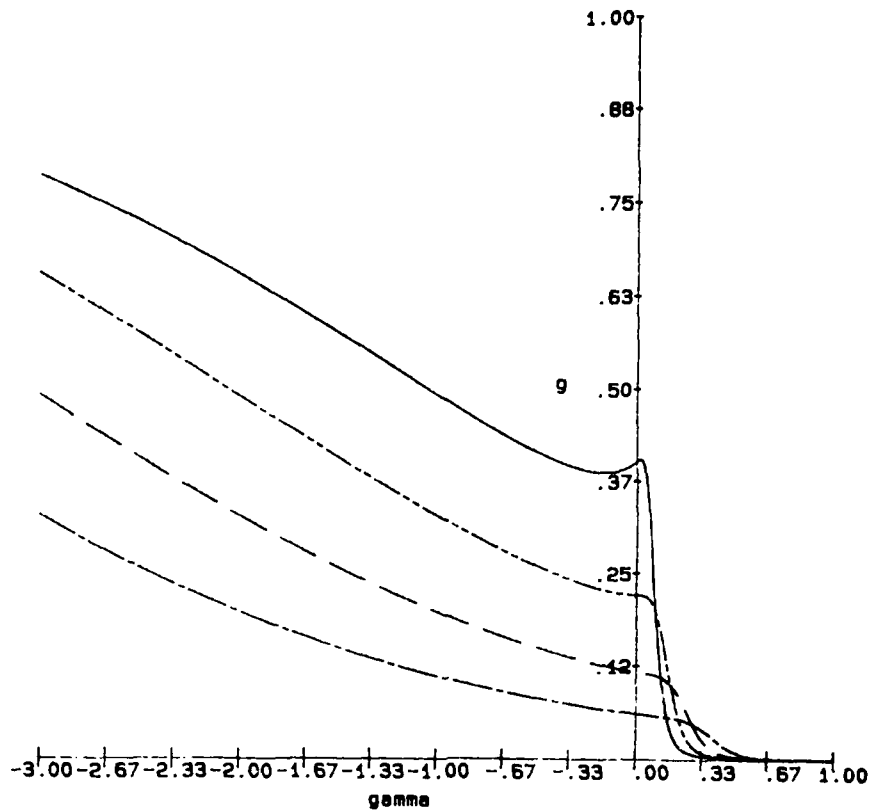
Figure 5. g versus $\log(\gamma)$ for a power-law material with $\epsilon=.01$, $n=.3$ and $\alpha=.1(\text{———})$, $1.0(\text{——·}$), $10.0(\text{— — —})$, $100.0(\text{—·—})$.

Figure 6.
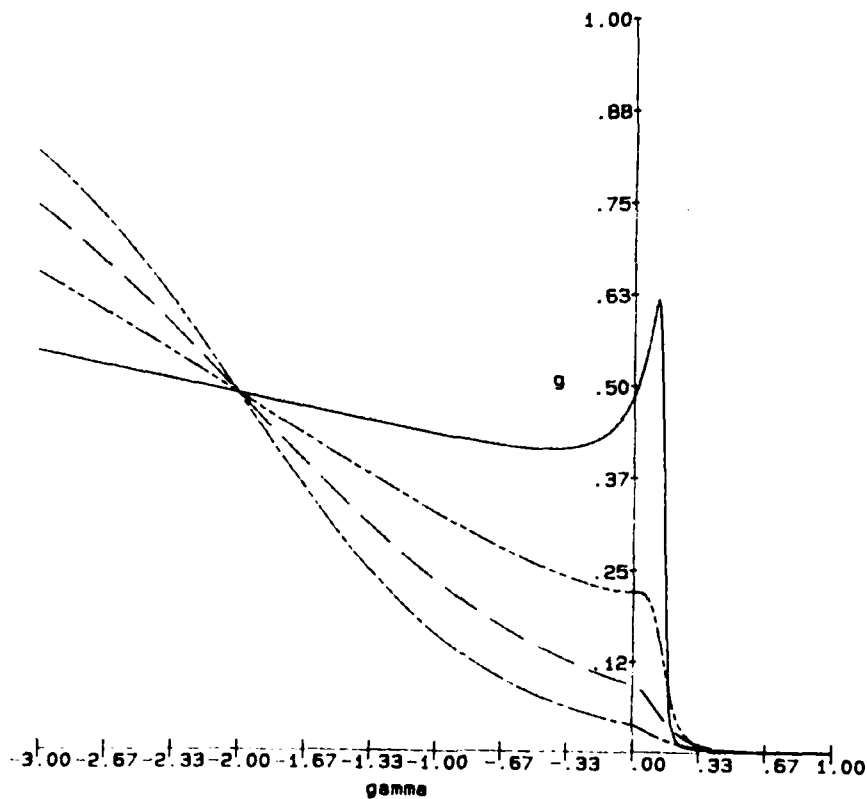
Figure 6. g versus $\log(\gamma)$ for a power-law material with $\epsilon=.01$, $\alpha=1.0$ and $n=.1(\text{———})$, $.3(\text{——·}$), $.5(\text{— — —})$, $.7(\text{—·—})$.

DTIC

END

4-86